Animal Nutrition 14 (2023) 130–140

Contents lists available at ScienceDirect

Animal Nutrition

journal homepage: http://www.keaipublishing.com/en/journals/aninu/

Original Research Article

Acid tolerance of lactate-utilizing bacteria of the order Bacteroidales contributes to prevention of ruminal acidosis in goats adapted to a high-concentrate diet

Zhongyan Lu [a], Lingmeng Kong [b], Shenhao Ren [b], Jörg R. Aschenbach [c, *], Hong Shen [b, d, *]

[a] Key Lab of Animal Physiology and Biochemistry, College of Veterinary Medicine, Nanjing Agricultural University, Nanjing, Jiangsu, China
[b] College of Life Science, Nanjing Agricultural University, Nanjing, Jiangsu, China
[c] Institute of Veterinary Physiology, Freie Universität Berlin, Berlin, Germany
[d] Bioinformatics Center, Academy for Advanced Interdisciplinary Studies, Nanjing Agricultural University, Nanjing, Jiangsu, China

ARTICLE INFO

Article history:
Received 9 March 2022
Received in revised form
7 April 2023
Accepted 11 May 2023
Available online 16 May 2023

Keywords:
Ruminal microbiome
Ruminal acidosis
Acid tolerance
Lactate metabolism

ABSTRACT

The rapid accumulation of organic acids, particularly lactate, has been suggested as the main cause of ruminal acidosis (RA) for ruminants fed high-concentrate diets. Previous research has shown that a gradual shift from low-to high-concentrate diets within 4 to 5 weeks effectively reduces the risk for RA. However, the mechanisms remain unknown. In this study, 20 goats were randomly allocated into four groups ($n = 5$) and fed with a diet containing a weekly increasing concentrate portion of 20%, 40%, 60%, and 80% over 28 d. At d 7, 14, 21, and 28, one group (named C20, C40, C60, and C80 according to the last concentrate level that they received) was killed and the ruminal microbiome was collected. Ruminal acidosis was not detected in any of the goats during the experiment. Nonetheless, ruminal pH dropped sharply from 6.2 to 5.7 ($P < 0.05$) when dietary concentrate increased from 40% to 60%. A combined metagenome and metatranscriptome sequencing approach identified that this was linked to a sharp decrease in the abundance and expression of genes encoding nicotinamide adenine dinucleotide (NAD)-dependent lactate dehydrogenase (nLDH), catalyzing the enzymatic conversion of pyruvate to lactate ($P < 0.01$), whereas the expression of two genes encoding NAD-independent lactate dehydrogenase (iLDH), catalyzing lactate oxidation to pyruvate, showed no significant concomitant change. Abundance and expression alterations for nLDH- and iLDH-encoding genes were attributable to bacteria from Clostridiales and Bacteroidales, respectively. By analyzing the gene profiles of 9 metagenome bins (MAG) with nLDH-encoding genes and 5 MAG with iLDH-encoding genes, we identified primary and secondary active transporters as being the major types of sugar transporter for lactate-producing bacteria (LPB) and lactate-utilizing bacteria (LUB), respectively. Furthermore, more adenosine triphosphate was required for the phosphorylation of sugars to initiate their catabolic pathways in LPB compared to LUB. Thus, the low dependence of sugar transport systems and catabolic pathways on primary energy sources supports the acid tolerance of LUB from Bacteroidales. It favors ruminal lactate utilization during the adaptation of goats to a high-concentrate diet. This finding has valuable implications for the development of measures to prevent RA.

1. Introduction

High-concentrate (HC) diets can induce ruminal acidosis (RA) characterized by daily episodes of ruminal pH drops to levels that impair ruminal physiological functions (pH < 5.6) such as the impairment of ruminal digestion, feed intake, and performance. Because HC diets are widely used in ruminants, RA ranks as the most important metabolic disorder of ruminant livestock (Plaizier et al., 2018). An imbalance between lactate-producing bacteria

* Corresponding authors.
E-mail addresses: Joerg.Aschenbach@fu-berlin.de (J.R. Aschenbach), hongshen@njau.edu.cn (H. Shen).
Peer review under responsibility of Chinese Association of Animal Science and Veterinary Medicine.

Production and Hosting by Elsevier on behalf of KeAi

https://doi.org/10.1016/j.aninu.2023.05.006

(LPB) and lactate-utilizing bacteria (LUB) has been suggested as the main cause of RA because it facilitates the rapid accumulation of organic acids (OA), particularly lactate, with negative consequences for the rumen buffering capacity (Aschenbach et al., 2011). Previous studies have shown that a gradual shift from a low-to high-concentrate diet (GSLHCD) over 4 to 5 weeks can effectively reduce the RA risk (Bevans et al., 2005; Humer et al., 2018). A functional adaptation of the ruminal microbiome to an HC diet, indicated by stable changes of the ruminal microbiome after GSLHCD, has been suggested to play an important role in the prevention of RA (Fernando et al., 2010; Hook et al., 2011). However, the time course of compositional and functional changes during the adaptation of the ruminal microbiome to an HC diet remains largely unknown, especially with regard to lactate metabolism.

Lactate metabolism includes lactate production and lactate utilization by LPB and LUB, respectively. Lactate dehydrogenase (LDH) enzymes catalyze the inter-conversion of pyruvate and lactate by both LPB and LUB. To date, two types of LDH have been reported, i.e., respiratory nicotinamide adenine dinucleotide (NAD)-independent LDH (iLDH) and fermentative NAD-dependent LDH (nLDH) (Garvie, 1980). Of these, iLDH has been shown to encode enzymes for lactate oxidation to pyruvate. It is coupled to an electron transport chain (ETC) that transfers electrons obtained from lactate oxidization to intracellular or extracellular oxides and generates the transmembrane electrochemical potential ($\Delta\mu H^+$/$\Delta\mu Na^+$) that, in turn, drives the production of adenosine triphosphate (ATP) (Kato et al., 2010; Pinchuk et al., 2009). Isoforms of nLDH have been demonstrated to catalyze the reduction of pyruvate to lactate, coupled to the regeneration of NAD^+ that is required for the sustenance of glycolysis (Zhao et al., 2013). So far, our understanding of the kinds of bacteria contributing to ruminal lactate metabolism is incomplete (Al Jassim et al., 2003; Hook et al., 2011). To unravel the adaptation of the ruminal microbiome to an HC diet from the perspective of lactate metabolism, we investigated the compositional and functional changes of LUB and LPB during GSLHCD by using a combined metagenome and metatranscriptome sequencing approach. The results are expected to support the development of cost-effective measures for the prevention of RA in the future.

2. Materials and methods

2.1. Ethics approval and consent to participate

All animal experiments complied with the ARRIVE guidelines and were carried out in compliance with the Regulations for the Care and Use of Animals of Nanjing Agricultural University (2018).

2.2. Animals and diets

Twenty goats (Boer × Yangtze River Delta White, 4 months old, 14 to 16 kg bodyweight) fitted with a permanent ruminal cannula were housed in individual pens (2 m × 2.5 m) and had free access to the tap water. After a 14-d adaptation to a hay diet, the goats were randomly allocated into four groups ($n = 5$). During the 28-d experimental period, the goats were fed with a diet containing increasing concentrate proportions of 20%, 40%, 60%, and 80% (i.e., increased by 20% per week, Table S1). At d 7, 14, 21, and 28, one group (named according to the last concentrate level that they received, i.e., C20, C40, C60, and C80) was killed at the local slaughterhouse 3 h after receiving their morning feed. To avoid feed sorting by animals, a total mixed ration (TMR) was individually provided twice daily at 07:00 and 16:00. The daily feed intake (DFI) by individual goats was measured.

Feeds were sampled at d 1 and 28 for chemical analysis. The dry matter (DM) content of feed samples was determined by drying them at 105 °C for 2 h, and the ash content was determined by combustion at 550 °C for 4 h (AOAC, 2019). Nitrogen concentration was determined by a Kjeltec Auto Analyzer (KDY-9820, Hengxiangtai Technology Co., Ltd, Tianjing, China), and then, crude protein (CP) content was calculated by multiplying the N concentration by 6.25. The ether extract (EE) content was determined by a Soxtec Auto Analyzer (ST-600, Zhiyue Scientific Instrument Co., Ltd, Shanghai, China). The contents of neutral detergent fiber (NDF) and acid detergent fiber (ADF) were determined according to the method described by Van Soest et al. (Van Soest et al., 1991).

2.3. Sample collection

To check whether RA occurred, ruminal fluid was collected for pH measurement through a rumen cannula at 0 h before morning feeding and at 2, 4, 6, 8, 12, and 14 h later for each goat from the 3rd to 7th day of the 3rd and 4th week of the experiment.

Immediately after slaughter, ruminal fluid was strained through a 4-layered cheese cloth, and fluid pH was determined by a pH meter (FE28, Mettler-Toledo Ltd., Shanghai, China). Subsequently, 20 mL ruminal fluid was collected per goat and stored at −20 °C for the extraction of microbial DNA and RNA. Another 20 mL ruminal fluid was mixed with 1 mL 5% $HgCl_2$ solution to inactive microbial proteases and stored at −20 °C for the later determination of the concentrations of ammonia nitrogen, short-chain fatty acids (SCFA), and lactate.

2.4. Ruminal ammonia, lactate, and SCFA concentration analysis

The concentrations of ruminal SCFA were determined by means of a gas chromatograph (HP6890N, Agilent Technologies, Wilmington, DE, USA) as described by Yang et al. (2012). The concentrations of L-lactate, D-lactate and ammonia nitrogen were determined with L-Lactate, D-Lactate, and Ammonia Assay Kits (ab65331, ab83429, and ab83360, Abcam Trading Company Ltd, Shanghai, China), respectively, and a microplate reader (Infinite M200 PRO, Tecan Trading AG, Switzerland).

2.5. Metagenome and metatranscriptome sequencing

Total DNA and RNA of the ruminal microbiome were extracted from the ruminal fluid with a Bacterial DNA Kit (Omega Bio-Tek, Shanghai, China) and a Mobio RNA PowerSoil® Total RNA Isolation Kit (Anbiosci Tech Ltd, Shenzhen, Guangdong, China), respectively. The concentrations of DNA and RNA were determined in a Nanodrop 1000 (Thermo Fisher Scientific Inc., Wilmington, DE, USA), and their integrity was evaluated on a 1.0% agarose gel. DNA libraries were constructed by using the TruSeq DNA Sample Prep Kit (Illumina, San Diego, CA, USA). Following the removal of rRNA by rRNA capture probes and magnetic beads, mRNA libraries were constructed by means of the TruSeq Stranded mRNA LT Sample Prep Kit (Illumina). The quality of each library was evaluated in a Bioanalyzer 2100 (Agilent Technologies, Santa Clara, CA, USA), and the quantity was evaluated in a QuantiFluor Fluorometer E6150 (Promega Corporation, Madison, Wisconsin, USA). Both DNA and RNA libraries were sequenced via paired-end chemistry (PE150) on an Illumina HiSeq X Ten platform at Biomarker Technologies, Beijing, China. The metagenome and metatranscriptome sequences are deposited at the National Center for Biotechnology Information (NCBI) under BioProject PRJNA757183.

2.6. Taxonomy, gene abundance and gene expression profiles analysis

Raw DNA and RNA reads were filtered by using Trimmomatic v0.40 (Bolger et al., 2014), with a quality cutoff of 20. Reads shorter than 50 bp were discarded from the sample. RNA reads were further preprocessed by means of SortMeRNA v4.3.4 (Kopylova et al., 2012) to remove the remaining rRNA fraction from the metatranscriptome data.

Taxonomy profiles of the ruminal microbiome were obtained via the individual assignments of the high-quality DNA reads to the relevant taxa via Kaiju v1.7.4 (Menzel et al., 2016) and the NCBI RefSeq reference database (updated on March 2021). A 20-metagenome co-assembly and 20 single-metagenome assemblies were carried out by using MEGAHIT v1.2.9 (Li et al., 2015). The genes were predicted from the co-assembled contigs by FragGeneScan 1.3 (Rho et al., 2010). CD-HIT v4.8.1 (Fu et al., 2012) was employed to construct the non-redundant coding genes (NCD) set with the parameters of 98% identity and 90% coverage of longer reads. High-quality DNA reads were individually mapped to the NCD by using Bowtie2 v2.4.4 (Langmead and Salzberg, 2012), and subsequently, HTSeq v0.13.5 (Anders et al., 2015) was employed to calculate the gene count of each sample. The transcripts per kilobase of exon model per million mapped reads (TPM) of the gene, calculated as [(gene count/gene length) $\times$ 10^6/sum (gene count/gene length)], were used to normalize the gene abundance (GA) within and between samples. The calculation of abundances (TPM) of contigs was consistent with that of genes. The predicted genes were blasted with the Kyoto Encyclopedia of Genes and Genomes (KEGG) Orthology (KO) databases to obtain KO and enzyme commissions (EC) numbers by using the KEGG Automatic Annotation Server (KAAS) (Moriya et al., 2007). High-quality mRNA reads were individually mapped to the NCD and genes of co-assembled contigs to obtain gene expression (GE) and contig expression values (TPM) by using Bowtie2.

Genes with significantly different abundance and expression between groups were used to analyze gene and transcript enrichments of KEGG metabolic pathways and KEGG transporter brites.

2.7. Phylogenetic analysis of ruminal LPB and LUB

Genes encoding nLDH, including NAD-depended L-lactate dehydrogenase gene (*ldh*, K00016) and NAD-depended D-lactate dehydrogenase gene (*ldhA*, K03778), and genes encoding iLDH, including cytochrome-dependent L-lactate dehydrogenase gene (*lldD*, K00101), quinone-dependent L-lactate dehydrogenase complex proteins genes (*lldE*, K18928; *lldF*, K18929; *lldG*, K00782), FAD-dependent D-lactate dehydrogenase gene (*dldII*, K18930), quinone-dependent D-lactate dehydrogenase gene (*dld*, K03777), and cytochrome-dependent L-lactate dehydrogenase gene (*dldH*, K00102), were searched for within the metagenome data. Finally, *ldh*, *ldhA*, *lldEFG* and *dldII* were detected (GA > 0.1 in at least one group) in the data.

Available gene sequences of the above four types of LDH were downloaded from UniProt databases and subsequently aligned with corresponding gene sequences detected in this study by using MAFFT v7.486 (Katoh and Standley, 2013). Maximum likelihood trees of each investigated LDH were constructed by means of the GTR model in PhyML v3.0 (Guindon et al., 2010). Taxonomy classifications of these genes were retrieved according to the Kaiju annotation results of co-assembled contigs with these genes.

2.8. Metabolic pathway and transport system analysis of ruminal LPB and LUB

Metagenomic bins (MAG) were predicted from both co-assembled and single-assembled contigs by using MetaBAT2 v2.15 (Kang et al., 2019). Received MAG were gathered together to delete replicated MAG by using dRep v3.0.1 (Olm et al., 2017) and CheckM v1.1.3 (Parks et al., 2015). Those replicated MAG with a completeness >80%, contamination <10%, and strain heterogeneity <10% were considered to be of high quality. Subsequently, high-quality MAG containing any genes for LDH were selected as representative of L-lactate-producing bacteria (L-LPB), D-lactate-producing bacteria (D-LPB), L-lactate-utilizing bacteria (L-LUB), and D-lactate-utilizing bacteria (D-LUB) in the analysis of metabolic pathways and transport systems of ruminal LPB and LUB. The gene prediction and KO assignment of these MAG were consistent with those of the contigs.

2.9. Statistical analysis

Unpaired two-tailed *t*-test was used for the analysis of DFI within each group among weeks and also for the analysis of ruminal pH, ammonia nitrogen, lactate, and SCFA concentrations among groups. Analysis of variance (ANOVA) was used for the analysis of DFI of each week among groups. Differences were considered significant when $P < 0.05$. Wilcoxon rank-sum test was used for the analysis of both GA and GE among groups. Differences were considered significant when false discovery rate (FDR) < 0.05 and $|\log_2| > 0.5$. The hypergeometric test was used in the enrichment analysis of both KEGG metabolic pathways and KEGG transporter brites. Differences were considered significant when FDR < 0.05. The statistical analyses were performed by R v4.2.0.

3. Results

3.1. Feed intake

During the experimental period, differences of DFI were not significant among the groups (Table S2). However, DFI decreased significantly in the C80 group from 2nd to 3rd week and from 3rd to 4th week. In the C60 group, DFI decreased significantly from 2nd to 4th week.

3.2. Ruminal pH and concentrations of ruminal lactate, SCFA, and ammonia nitrogen

During the experimental period, a pH < 5.6 was observed in 3/10 goats at 1 h after the morning feeding during the first 2 days of provision of the 60% concentrate diet and 2/5 goats at 1 h after the morning feeding during the first day of provision of the 80% concentrate diet.

In ruminal fluid samples taken immediately after slaughter, ruminal pH decreased significantly from C20 to C40 and from C40 to C60, without further decrease toward C80 (Fig. 1). In parallel, ruminal D-lactate, L-lactate, total lactate, and total SCFA showed significant increases from C20 to C40 and, additionally, from C40 to C60. Concentrations of acetate and propionate increased significantly from C40 to C60. Ammonia nitrogen concentration increased in two steps from C40 to C60 and from C60 to C80.

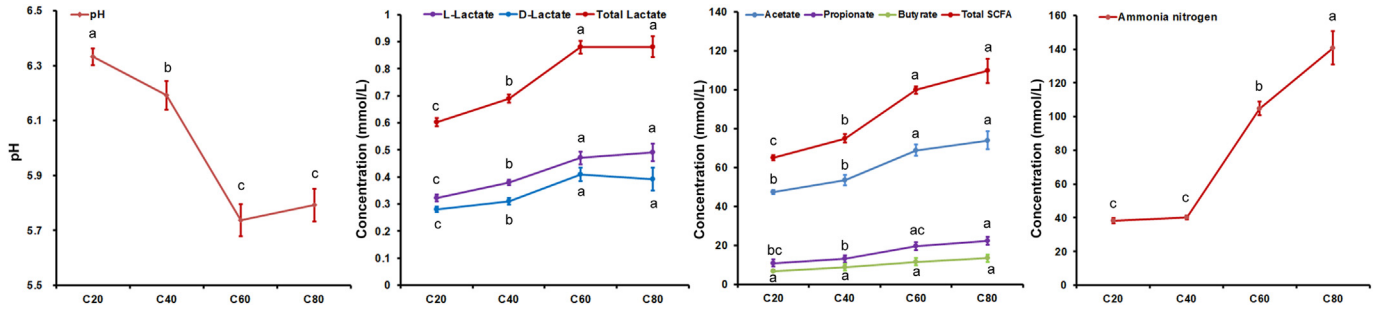

Fig. 1. Changes of ruminal fermentation variables in goats fed a diet containing a weekly increasing concentrate portion of 20% (C20), 40% (C40), 60% (C60), and 80% (C80). [a-c] Different letters indicate differences among groups at $P < 0.05$ in the paired two-tailed *t*-test.

3.3. Microbial composition

Analysis of the microbial composition obtained via an unassembled classification method revealed that the relative abundance of Archaea significantly increased from C40 to C60 and from C60 to C80 (Fig. S1). The alpha diversity of the microbial community, indicated by the Shannon index, and the richness of microbes within the community, indicated by the dilution curve, were C20 = C40 > C60 = C80 (Fig. S1).

With regard to changes of the relative abundance of the six prevalent phyla whose relative abundance was more than 1% in at least one group, we found that 1) Firmicutes showed changes that were similar to those of ruminal pH; 2) Bacteroidetes, Actinobacteria, and Spirochaetes exhibited the highest values in C40; 3) the values of Proteobacteria and Euryarchaeota were higher in C60 and C80 than in C20 and C40 (Fig. S2). With regard to changes of the relative abundance of the 16 prevalent genera whose relative abundance was more than 0.1% in at least one group, we determined that 1) all four genera from the order Clostridiales (*Eubacterium*, *Ruminococcus*, *Clostridium*, and *Butyrivibrio*) showed a sharp decrease from C20 to C40; 2) values for *Bacteroides*, *Treponema*, and *Alistipes* were the highest in C40, values for *Prevotella*, *Succinimonas*, *Selenomonas*, and *Fibrobacter* were the highest in C60, whereas values for *Succiniclasticum*, *Methanobrevibacter*, and *Succinivibrio* were the highest in C80 (Fig. S2).

3.4. Microbial metabolic pathways

Metabolic pathways that differed among groups in the enrichment analysis are presented in Fig. 2. With regard to carbohydrate metabolism, five major sugar catabolic pathways of ruminal microbes, i.e., glycolysis, the pentose phosphate pathway (PPP), the Entner–Doudoroff (ED) pathway (embedded in the galactose metabolic pathway), inositol phosphate metabolism and butanoate metabolism exhibited significant differences from C20 to C40, with some also displaying significant differences from C40 to C60 and from C60 to C80 at the GA level. Only butanoate metabolism showed significant differences from C20 to C80 at the GE level. Within amino acid (AA) metabolism, seven pathways showed significant differences from C20 to C40, with four of them displaying significant differences from C40 to C60 at the GA level. Only one pathway showed significant differences from C40 to C60 at the GE level. Within lipid metabolism, fatty acid (FA) degradation and glycerolipid metabolism exhibited significant differences from C20 to C40 at the GA level. However, none of them showed significant differences at the GE level. Significant differences were detected in methane metabolism from C20 to C40 and from C40 to C60 at the GA level and from C40 to C60 at the GE level.

3.5. Microbial transport systems

The detected transporters were allocated to 28 categories according to the driving force (ATP, phosphoenolpyruvate [PEP], electrochemical potential and ion concentration gradient; for details, see Transporter Classification Database: http://www.tcdb.org/index.php) and the transported substrates (i.e., carbon source, nitrogen source, lipids, ion, and others). The enrichment analysis of the 28 categories is shown in Fig. 2. With regard to the transportation of carbon source substrates, ATP-binding cassette (ABC) transporters [TC:3.A.1], PEP-dependent phosphotransferase systems (PTS) [TC:4. A], and major facilitator superfamily (MFS) porters [TC:2.A.1] showed significant differences from C40 to C60 at the GA level. The MFS porters and electrochemical potential-driven transporters (EPDT) [TC:2] exhibited significant differences from C20 to C40 at the GA level. Only ABC transporters showed significant differences from C40 to C60 and from C60 to C80 at the GE level. With regard to the transportation of nitrogen source substrates, ABC transporters, PTS, and EPDT exhibited significant differences from C20 to C40, and the former was associated with a significant difference from C40 to C60 at the GA level. ABC transporters and EPDT showed significant differences from C40 to C60 at the GE level. With regard to the transportation of lipids, ABC transporters and MFS porters displayed significant differences from C20 to C40, and the former was associated with significant difference from C40 to C60 and from C20 to C80 at the GA level. With regard to the transportation of ions, ABC transporters, EPDT, and the pore ion (PI) category [TC:1] exhibited significant differences from C20 to C40 and/or from C40 to C60 at the GA level. ABC transporters and EPDT showed significant differences from C40 to C60 at the GE level.

3.6. Abundance and expression of LDH-encoding genes and microbes with LDH-encoding genes

The abundance of all genes encoding LDH peaked at C40 and showed significant decreases from C60 to C80. The abundance of *ldh*, *ldhA*, and *lldEFG* (derived from the mean values of the three subunits *lldE, lldF and lldG*) exhibited significant decreases from C40 to C60 (Fig. 2). The expression of *ldh* and *ldhA* decreased significantly from C40 to C60. However, the expression of *lldEFG* and *dldII* displayed no significant changes from C40 to C60.

Genes encoding LDH were contained in a total of 167 contigs with *ldh* (L-LPB), 175 contigs with *ldhA* (D-LPB), 114 contigs with *lldE*, 167 contigs with *lldF*, 49 contigs with *lldG*, and 185 contigs with *dldII* (D-LUB). Since 97% of contigs with *lldE* and 92% contigs with *lldG* were covered by the contigs with *lldF*, only *lldF* was used in the analysis of phylogenetic relationships of species with *lldEFG* (L-LUB).

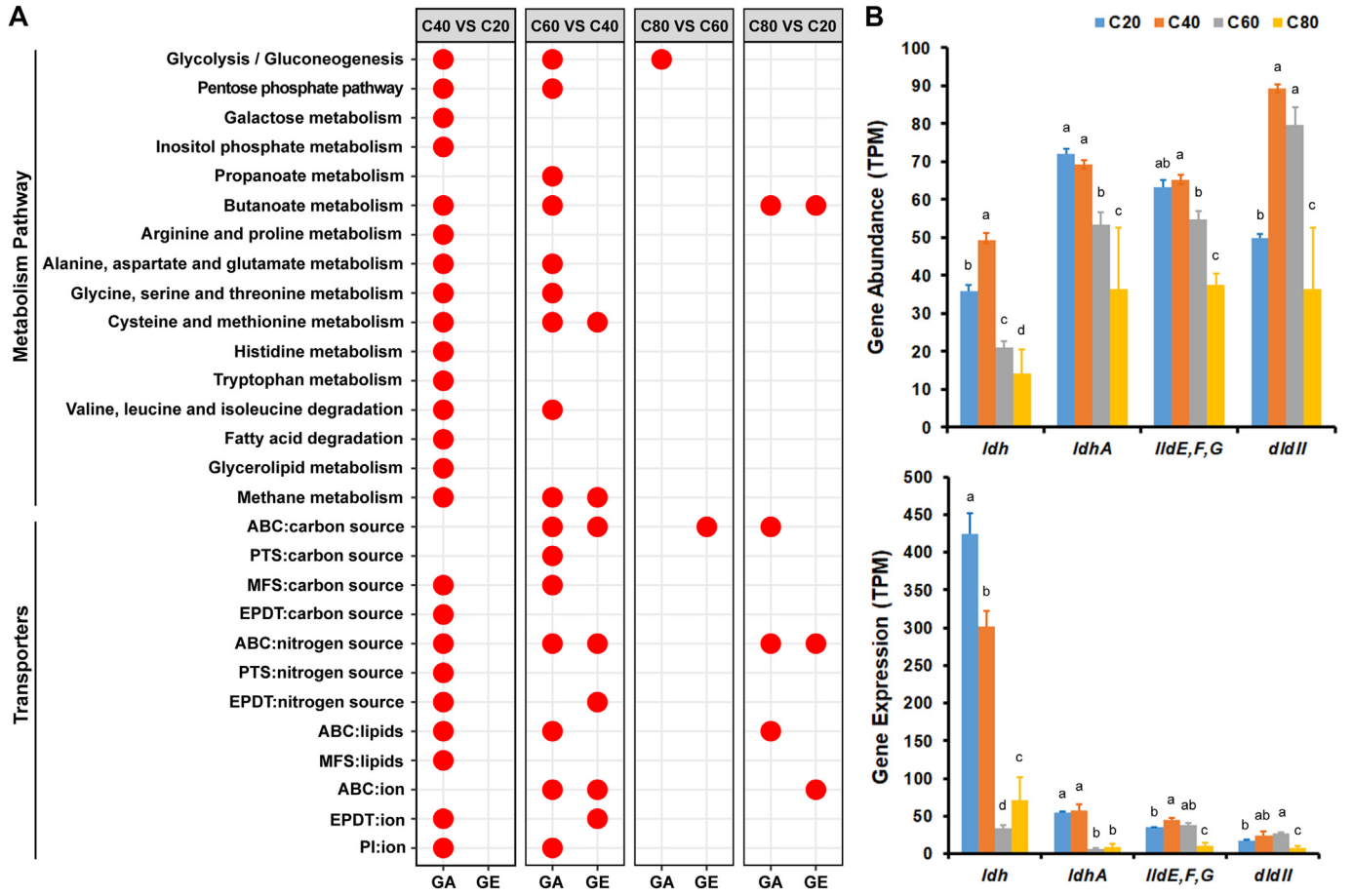

Fig. 2. Influence of a gradual shift from a low-to high-concentrate diet on bacterial gene and transcript pool. (A) Enrichment analysis of the metabolic pathways and transporter systems. (B) Changes of the lactate dehydrogenase (LDH) genes. [a-d] Different letters indicate differences among groups at a false discovery rate (FDR) < 0.05 in the Wilcoxon rank-sum test. ABC = adenosine triphosphate-binding cassette; PTS = phosphoenolpyruvate-dependent phosphotransferase system; MFS = major facilitator superfamily; EPDT = electrochemical potential-driven transporter; TPM = transcripts per kilobase of exon model per million mapped reads; *ldh* = gene encoding nicotinamide adenine dinucleotide (NAD)-depended L-LDH; *ldhA* = gene encoding NAD-depended D-LDH; *lldD* = gene encoding cytochrome-dependent L-LDH; *lldE, F, G* = quinone-dependent L-LDH complex proteins genes.

Eight clades of L-LPB could be identified in the present study within the phylogenetic tree of *ldh*-containing microbes (Fig. 3). Four of these clades accounted for >80% of L-LPB counts: three clades with species belonging to the order Clostridiales (referred to as O_Clostridiales_I, O_Clostridiales_II, and O_Clostridiales_III) and one clade with species belonging to the genus *Selenomonas* (G_*Selenomonas*) accounted for 15.0%, 14.3%, 40.1%, and 13.8% of total L-LPB counts, respectively. The abundance of clades (calculated by the abundance of *ldh*-containing contigs within a clade) decreased significantly for O_Clostridiales_II, III, O_Rhodospirillales, and C_Alphaproteobacteria from C40 to C60, whereas G_*Methanobrevibacter* showed a significant increase. Except for C_Alphaproteobacteria, none of the clades showed a significant increase from C60 to C80. The expression of clades (calculated by the expression of *ldh*-containing contigs within a clade) largely followed the changes of ruminal pH among groups.

Six clades of D-LPB were identified in the phylogenetic tree of *ldhA*-containing microbes (Fig. 3). The two most abundant clades belonged to the order Clostridiales, accounting for 36.0% (O_Clostridiales_I) and 43.4% (O_Clostridiales_II) of total D-LPB counts. Although nine genera were found to be shared by these clades with the O_Clostridiales_I, II, III in the *LdhA* tree, no single species (contig) was found to contain both *ldh* and *ldhA*. One clade consisting of species belonging to the genus *Prevotella* (G_*Prevotella*) accounted for 12.6% of total D-LPB counts. In response to GSLHCD, the abundance and expression of O_Clostridiales_I and O_Clostridiales_II showed a significant decrease from C40 to C60. G_*Prevotella* exhibited a significant increase in C20 to C40 and a significant decrease from C60 to C80.

From the phylogenetic tree of *lldF*, eight clades of L-LUB were identified in the dataset (Fig. 3). One clade with species from the genus *Prevotella* (G_*Prevotella*) accounted for 67.7% of total L-LUB counts, and one clade with species from the order Bacteroidales (O_Bacteroidales) accounted for 9.9% of total L-LUB counts. The abundance of G_*Prevotella* displayed a significant decrease from C40 to C60 and from C60 to C80, paralleled by a significant decrease in expression from C60 to C80. For O_Bacteroidales, a significant decrease in abundance and expression was seen from C40 to C60.

Within the phylogenetic tree of *dldII*, all identified D-LUB belonged to two clades of the order Bacteroidales (O_Bacteroidales_I and II), accounting for 39.5% and 60.5% of total D-LUB counts, respectively (Fig. 3). The genus *Prevotella* was shared by these clades of O_Bacteroidales. However, no single species (contig) contained both *lldF* and *dldII*. In response to GSLHCD, the abundance and expression of O_Bacteroidales_I and O_Bacteroidales_II showed a significant decrease from C60 to C80.

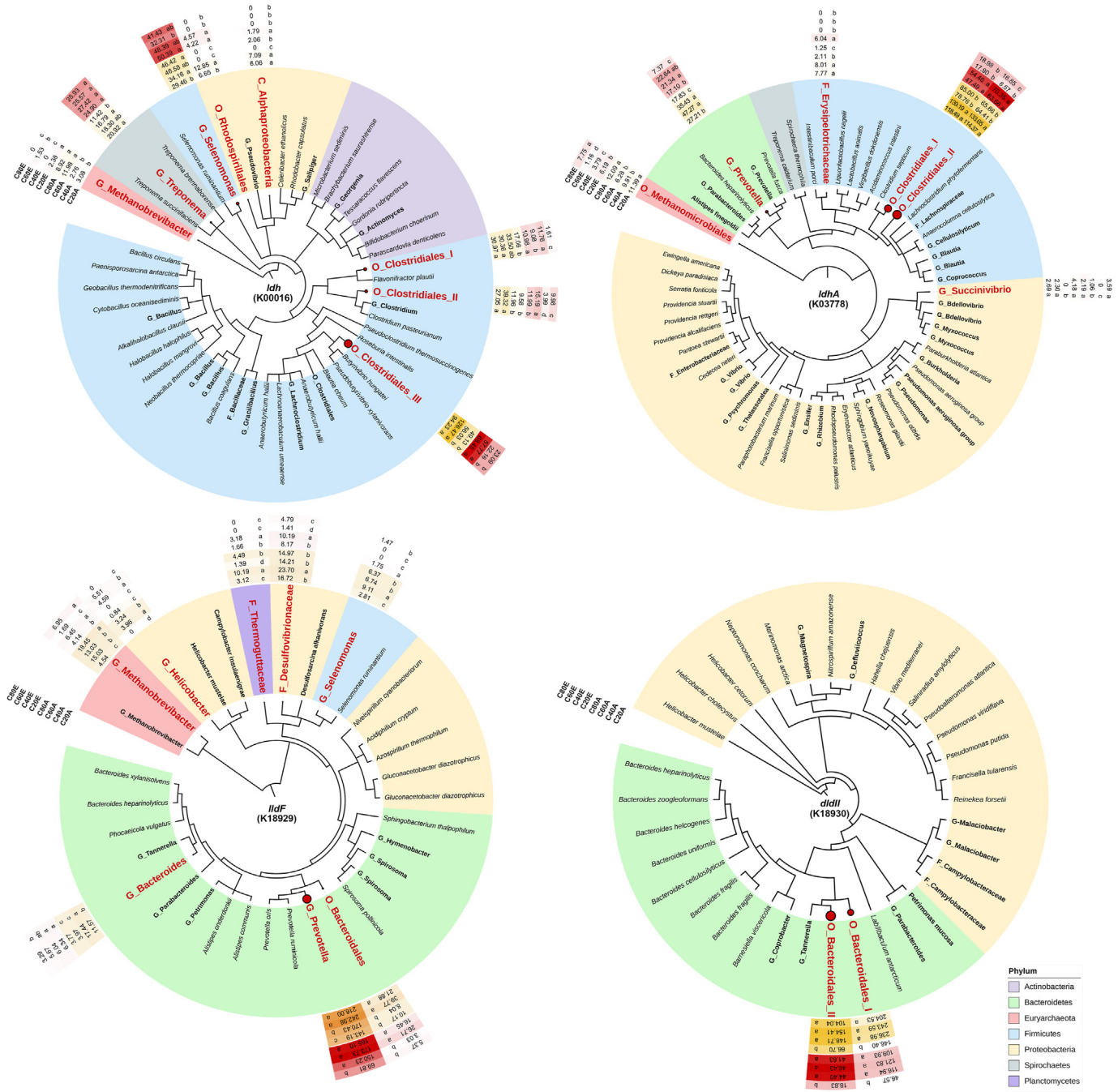

Fig. 3. Phylogenetic relationships of lactate-producing bacteria (LPB) and lactate-utilizing bacteria (LUB) constructed from the genes encoding lactate dehydrogenase (LDH) detected in this study and the corresponding LDH in the UniProt datasets. Heat maps next to the clades show the changes of abundance (in yellow) and expression (in red) of clades containing the corresponding contigs with LDH-encoding genes among groups. [a-d] Different letters indicate differences among groups at a false discovery rate (FDR) < 0.05 in the Wilcoxon rank-sum test.

3.7. Differences in transport systems and sugar catabolic pathways of 14 high-quality MAG with genes encoding LDH

In total, 140 high-quality MAG were obtained in this study. Among them, five, four, four, and one MAG were found to contain *ldh*, *ldhA*, *lldF*, and *dldII*, respectively (Table 1). A comparison of transporters for carbon source substrates among 14 MAG revealed that ABC transporters and PTS were the major types for all LPB, whereas MFS porters, PI, and EPDT were the major types for all LUB from the order Bacteroidales (Fig. 4). Within LPB, D-LPB had more genes for MFS porters, PI, and EPDT than did L-LPB. The fewest numbers of transporters for carbon source substrates were detected in two C_Alphaproteobacteria and in *Methanobrevibacter wolinii*. In the comparisons of transporters for nitrogen source substrates, ABC transporters and PTS were significantly more prevalent in LPB compared with LUB. However, the prevalence of PI and EPDT showed no significant difference between LPB and LUB. In the comparisons of transporters for lipids, more transporters were found in LUB (with the exception of *M. wolinii*) than in LPB (with the exception of C_Alphaproteobacteria). No significant difference

Table 1
High-quality metagenome bins (MAG) with lactate dehydrogenase genes (LDH).

Item	MAG	LDH Gene	Clade on Tree
L-LPB	G_*Butyrivibrio*	*ldh*	O_Clostridiales_III
	G_*Oscillibacter*	*ldh*	O_Clostridiales_III
	C_Alphaproteobacteria	*ldh*	C_Alphaproteobacteria
	C_Alphaproteobacteria	*ldh*	C_Alphaproteobacteria
	Treponema bryantii	*ldh*	G_*Treponema*
D-LPB	G_*Clostridium*	*ldhA*	O_Clostridiales_I
	G_*Ruminococcus*	*ldhA*	O_Clostridiales_II
	G_*Ruminococcus*	*ldhA*	O_Clostridiales_II
	Succinivibrio dextrinosolvens	*ldhA*	G_*Succinivibrio*
L-LUB	O_Bacteroidales	*lldE; lldF*	O_Bacteroidales
	G_*Prevotella*	*lldE; lldF*	G_*Prevotella*
	Desulfovibrio fairfieldensis	*lldF*	F_Desulfovibrionaceae
	Methanobrevibacter wolinii	*lldF; lldG*	G_*Methanobrevibacter*
D-LUB	G_*Bacteroides*	*dldII*	O_Bacteroidales_II

L-LPB = L-lactate-producing bacteria; D-LPB = D-lactate-producing bacteria; L-LUB = L-lactate-utilizing bacteria; D-LUB = D-lactate-utilizing bacteria; G = genus; O = Order; C = Class; F = Family; *ldh* = gene encoding nicotinamide adenine dinucleotide (NAD)-depended L-LDH; *ldhA* = gene encoding NAD-depended D-LDH; *lldD* = gene encoding cytochrome-dependent L-LDH; *lldEFG* = genes encoding quinone-dependent L-lactate dehydrogenase complex proteins.

was detected in the types of transporters for ions between LUB and LPB.

Based on the KO composition and the substrates of carbon source transporters, we reconstructed the major sugar catabolic pathways for these 14 high-quality MAG (Fig. 5, Fig. S3 & Table S3). Six of 32 carbon sources were determined as being commonly used by LPB and LUB (black entry transporters and substrate letters in Fig. 5). In total, 13 sugars and five phosphorylated sugars (sugar-P) exclusively used by LPB (red entry transporters and substrate letters in Fig. 5) were degraded into pyruvate via glycolysis and PPP. Six out of 11 carbon sources exclusively used by LUB (blue entry transporters and substrate letters in Fig. 5) were degraded into pyruvate. From the remaining carbon source substrates used by LUB, inositol-P was converted into pyruvate via the ED pathway. Starch, transported by the TonB-dependent starch-binding outer membrane protein (T36) of LUB, and maltose-6P were degraded into pyruvate via complete glycolysis.

Acetate-CoA ligase (P36), lactaldehyde dehydrogenase (P37), L-fucose isomerase (PP28), and three enzymes of propionate metabolism (PP47-49) were not detected in any of the LPB. Succinyl-CoA synthetase (P23), formate C-acetyltransferase (P29), alcohol dehydrogenase (P34), aldehyde dehydrogenase (P35), seven enzymes in the initial catabolic pathways of sugars (PP1, 4, 6, 11, 13, 21, and 34), and two enzymes of butanoate metabolism (PP40 and 43) were not detected in any of the LUB. Additionally, six unspecific sugar transporters (T1, 2, 6, 16, 17, and 24) were present in LPB, and one unspecific sugar-P transporter was present in LUB (T32).

Functional responses of MAG to GSLHCD could not be determined because of the low abundance and expression of genes within each individual MAG.

4. Discussion

In this study, acute RA with ruminal pH < 5.0 or 5.2 and lactate concentration > 5 mmol/L (Nagaraja and Titgemeyer, 2007; Nocek, 1997) and subacute RA (SARA) with a duration of ruminal pH < 5.6 for more than 3 h/24 h (Plaizier et al., 2008) did not occur in any of the goats during the GSLHCD.

HC diets are known to promote the growth of amylolytic LPB in the rumen. The growth of LPB is favored by their acid tolerance, e.g.,

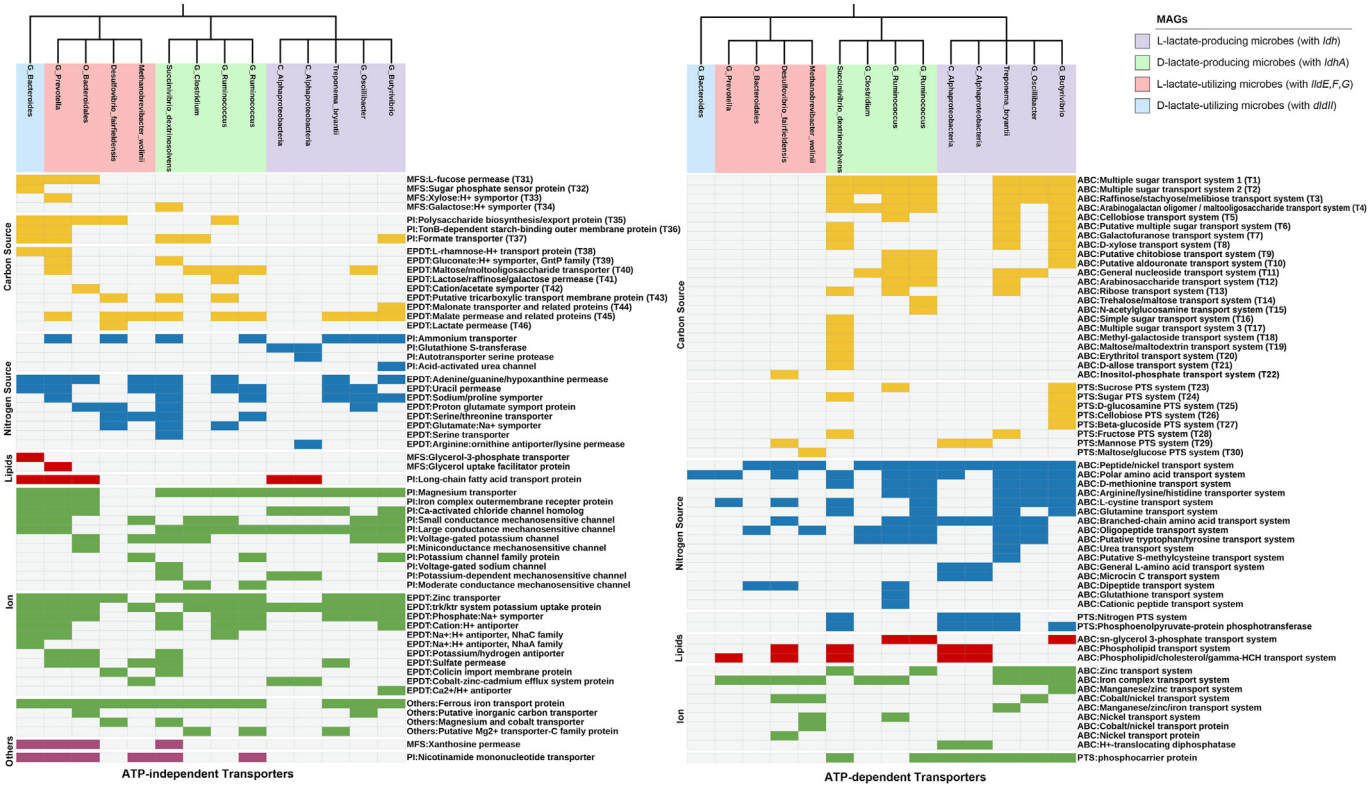

Fig. 4. Comparisons of the identified transporters for carbon sources, nitrogen sources, lipids, and ions between 14 high-quality metagenome bins with genes encoding lactate dehydrogenase. MFS = major facilitator superfamily; PI = pore ion; EPDT = electrochemical potential-driven transporter; ABC = adenosine triphosphate-binding cassette; PTS = phosphoenolpyruvate-dependent phosphotransferase system.

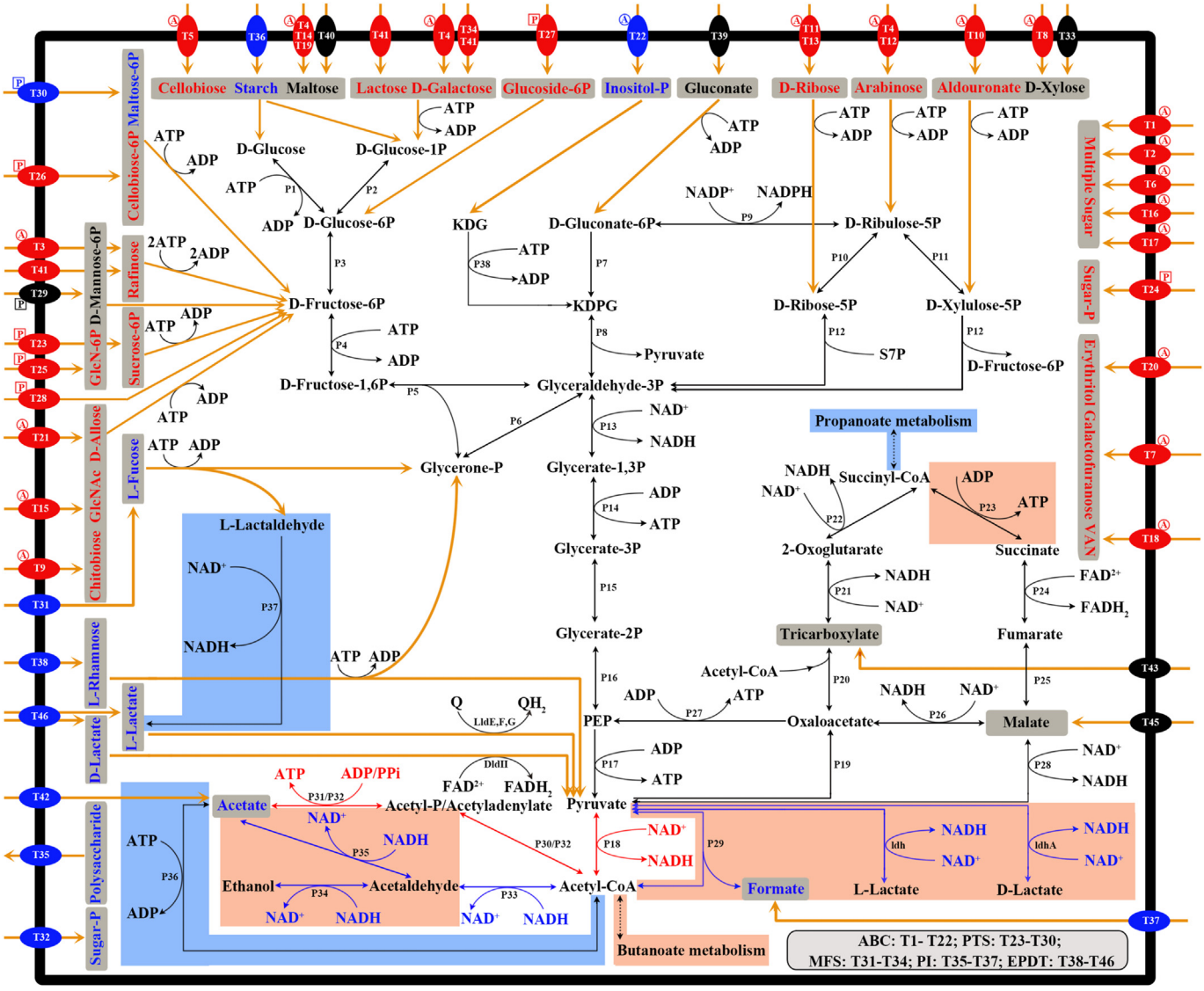

Fig. 5. Sugar catabolic pathways of 14 high-quality metagenome bins with genes encoding lactate dehydrogenase (LDH). Detailed information of the pathway enzymes is summarized in Table S3. Further details of pathways depicted by yellow arrows are presented in Fig. S3. Transporters with an attached A indicate adenosine triphosphate (ATP)-binding cassette (ABC) transporters that require ATP for the translocation of substrate, and transporters with an attached P indicate phosphoenolpyruvate (PEP)-dependent phosphotransferase systems (PTS) transporters that required PEP for the translocation of substrate. The colors red, blue, and black for transporters and substrates indicate that they were detected in lactate-producing bacteria (LPB), lactate-utilizing bacteria (LUB), and both, respectively. The pathway regions in orange and the blue boxes indicate that they were only found in LPB and LUB, respectively. The preferential conversion of pyruvate in LPB under acid stress and normal condition is symbolized by red and blue arrows, respectively. MFS = major facilitator superfamily; PI = pore ion; EPDT = electrochemical potential-driven transporter; *ldh* = gene encoding nicotinamide adenine dinucleotide (NAD)-depended L-LDH; *ldhA* = gene encoding NAD-depended D-LDH; *lldD* = gene encoding cytochrome-dependent L-LDH; *lldE, F, G* = quinone (Q)-dependent L-LDH complex proteins genes; VAN = methyl-beta-galactoside; GlcNAc = N-acetylglucosamine; FAD = flavin adenine dinucleotide.

pH approximately 4.8 for *Streptococcus bovis* (Russell and Dombrowski, 1980) or pH < 4.3 for *Lactobacillus* spp. (Long et al., 2009; Nagaraja and Titgemeyer, 2007), and appears to be greater than that of LUB, e.g., pH 5.6 for *Megasphaera elsdenii* (Russell and Dombrowski, 1980). This allows LPB to proliferate more rapidly than LUB when ruminal pH drops below 5.5 (Chen and Wang, 2016). A rapid increase of lactate without adequate consumption by LUB and absorption by the ruminal epithelium can lead to an increase of ruminal lactate concentration. Since the acidity of lactate is ten times that of SCFA, the increase of ruminal lactate concentration can promote a rapid reduction of ruminal pH (Aschenbach et al., 2011).

In the present study, ruminal lactate concentration stayed below 1 mmol/L, indicating that lactate production and lactate utilization were well balanced during GSLHCD. In LPB, the change of expression of genes encoding nLDH coincided with the change of ruminal pH, indicating sensitivity of nLDH-encoding gene expression to the ruminal pH in agreement with previous studies (Brown et al., 2006; Chen et al., 2019). With regard to the taxonomy of LPB, the majority belonged to the order Clostridiales and the genus *Selenomonas*, which were also the predominant taxa of LPB isolated from the rumen at low pH in a previous study (Hernandez et al., 2008). However, the changes the abundance of nLDH-encoding genes followed a bell-shaped curve with the highest values in C40 (Fig. 2), indicating that the growth of most LPB was initially promoted by dietary concentrate and later suppressed by low pH. In particular, the abundance and gene expression of LPB of the order Clostridiales sharply decreased

when dietary concentrate increased from 40% to 60% and ruminal pH dropped from 6.2 to 5.7 (Fig. 3). These results support a (relatively) low acid tolerance for LPB of the order Clostridiales. Earlier studies have demonstrated that acid stress inhibits the glycolytic pathway of LPB from the order Clostridiales and also decreases the capture of biochemical energy (Even et al., 2002). For the adaptation to acidic stress, LPB usually change the degradation pathway of pyruvate from lactate to acetate (Fig. 5) and reduce their growth and proliferation rate (Even et al., 2002; Konings et al., 1997). The switch of pyruvate degradation toward acetate has been suggested to decrease the intracellular stress level by the concurrent reduction of lactate production (Papadimitriou et al., 2016). The results of the present study additionally suggest that this switch also increases the production of ATP. The increased ATP availability would serve as an energy source for ABC transporters, which we have identified as the major sugar transporters in LPB of the order Clostridiales. Furthermore, ATP would encourage sugar phosphorylation in the initial phase of sugar catabolism, being important for the uptake and utilization of energy/carbon substrates by these LPB. Taken together, a suppression of lactate production and a reduction of growth of Clostridiales as the major LPB provide a plausible and important explanation for the maintenance of low ruminal lactate concentrations during GSLHCD.

In the present study, *Treponema* spp., which are proteolytic AA-fermenting anaerobes that are able to convert glycine into lactate (Tan et al., 2014), were notably the only L-LPB group whose expression showed no significant changes during GSLHCD. Thereby, *Treponema* spp. rose to the second highest expression level within L-LPB in C60 and C80, when Clostridiales were decreasing. The high acid tolerance of *Treponema* might be explained by the production of ammonia during AA and protein degradation as a common response of LPB to resist low pH (Papadimitriou et al., 2016).

The *dldII* and *lldEFG*, first identified in *Shewanella oneidensis* (Pinchuk et al., 2009), were determined as being the main genes encoding iLDH in the gene pool of caprine ruminal microbiota in the present study. Furthermore, bacteria from the order Bacteroidales were identified as the major microbes with *lldEFG* and the only microbes with *dldII*. Previously, *M. elsdenii* had been regarded as the predominant DL-LUB in the rumen based on lactate incubation and lactate infusion experiments (Counotte et al., 1981). However, recent studies revealed that *M. elsdenii* are rare in the rumen of healthy ruminants (Henderson et al., 2016; Jami and Mizrahi, 2012; Li et al., 2017; Xue et al., 2018) and even rare in the rumen of SARA-affected cattle with less than 1 mmol/L ruminal lactate concentration (Ogunade et al., 2019). One in vitro study demonstrated that the growth of *M. elsdenii* is greatly promoted by the increase of lactate concentration from 10 to 30 mmol/L, whereas it is little affected by a change of pH from 6.5 to 5.5 (Chen et al., 2019). Accordingly, we can speculate that relatively high lactate concentrations (>1 mmol/L) might be required to promote the growth of *M. elsdenii* in the rumen. Vice versa, the low ruminal lactate concentrations might explain the virtual absence of *M. elsdenii* during GSLHCD in the present study.

The abundance and expression of both *dldII* and LUB of the order Bacteroidales remained unchanged when the dietary concentrate portion increased from 40% to 60% and ruminal pH dropped from 6.2 to 5.7, indicating a higher acid tolerance of LUB of the order Bacteroidales. By comparing the gene profiles of LUB from the order Bacteroidales with those of LPB from the order Clostridiales, we found that more primary energy sources (ATP and PEP) were required for the translocation and catabolism of carbon sources by LPB than LUB based on the differences in transport systems and carbon source substrates. Accordingly, we suggest that the usage of secondary active transporters and lower ATP consumption by carbon substrates/sugar-P are supportive to a relatively high acid tolerance of LUB from the order Bacteroidales. Taking these data together, we suggest that the ATP/PEP-sparing transport systems and catabolic pathways for sugars support the high acid tolerance of LUB from the order Bacteroidales, contributing to the prevention of RA during GSLDH.

To date, most LUB isolated from rumen, such as *Selenomonas ruminantium*, *Propionibacterium shermanii*, and *Veillonella*, were shown to convert lactate into acetate and propionate via the succinate pathway (Counotte et al., 1981; Gilmour et al., 1996). In the present study, the succinyl-CoA synthetase (P23) gene of the succinate pathway was not detected in the sequences of LUB. As an alternative pathway, the conversion of succinyl-CoA into succinate was found to be catalyzed by an acetate:succinate CoA-transferase in *Acetobacter aceti* (Mullins et al., 2008; Mullins and Kappock, 2012), and a CoA transferase was proposed to catalyze the conversion of succinate to succinyl-CoA in *Clostridioides acetobutylicu* (Au et al., 2014) and the lactate-utilizing *Bacteroides fragilis* (Macy et al., 1978). Accordingly, we suggest that LUB of the order Bacteroidales also convert lactate into acetate and propionate via the succinate pathway, like most LUB in the rumen.

Finally, the metabolic functions of the whole microbial community, indicated by the results of pathway enrichment analysis on the GE level, changed little during GSLHCD, despite numerous changes in the pathway enrichment analyses on the GA level. This finding is only slightly surprising and points to the functional redundancy and anti-interference properties of the ruminal microbiome (Edwards et al., 2008). The latter aspect surely contributes to the maintenance of metabolic homeostasis in the rumen during the GSLHCD.

Among the measured parameters for rumen fermentation, ammonia concentration showed a sharp increase when the dietary concentrates increased from 40% to 60%. Previous studies showed that a moderate increase of dietary concentrate feed can promote the degradation of protein content in the rumen, leading to an increase of ruminal ammonia concentration (Zhou et al., 2015). Our previous ex vivo study indicated that, at low pH level, the increase of ruminal ammonia concentration promotes the uptake of ammonium (NH_4^+), and subsequently, stimulates proton extrusion via Na^+/H^+ exchange by the ruminal epithelial cells, leading to a further reduction of ruminal pH (Abdoun et al., 2005). Accordingly, we consider that the increased ammonia concentration contributes to the reduction of ruminal pH when the dietary concentrate portion increases from 40% to 60%.

5. Conclusions

Compared to the predominant LPB of the order Clostridiales, the predominant LUB of the order Bacteroidales show a higher acid tolerance and a lower dependence of sugar transport systems and catabolic pathways on primary energy sources in the caprine rumen during a GSLHCD. This indicates that the adaptations of these LPB and LUB are an important reason for the maintenance of ruminal lactate homeostasis during a GSLHCD.

Author contributions

Zhongyan Lu: Methodology, Investigation, Software, Data curation, Visualization, Writing – original draft. **Lingmeng Kong:** Methodology, Investigation. **Shenhao Ren:** Methodology. **Jörg R. Aschenbach:** Conceptualization, Writing – original draft, Writing – review & editing. **Hong Shen:** Conceptualization, Formal analysis, Writing – original draft, Writing – review & editing, Funding acquisition.

Declaration of competing interest

We declare that we have no financial and personal relationships with other people or organizations that can inappropriately influence our work, and there is no professional or other personal interest of any nature or kind in any product, service and/or company that could be construed as influencing the content of this paper.

Acknowledgements

This work was supported by the National Natural Science Foundation of China (31802155).

Appendix Supplementary data

Supplementary data to this article can be found online at https://doi.org/10.1016/j.aninu.2023.05.006.

References

Abdoun K, Stumpff F, Wolf K, Martens H. Modulation of electroneutral na transport in sheep rumen epithelium by luminal ammonia. Am J Physiol Gastrointest Liver Physiol 2005;289:G508–20.
Al Jassim RaM, Gordon GLR, Rowe JB. The effect of basal diet on lactate-producing bacteria and the susceptibility of sheep to lactic acidosis. Anim Sci 2003;77:459–69.
Anders S, Pyl PT, Huber W. Htseq–a python framework to work with high-throughput sequencing data. Bioinformatics 2015;31:166–9.
Aschenbach JR, Penner GB, Stumpff F, Gabel G. Ruminant nutrition symposium: role of fermentation acid absorption in the regulation of ruminal ph. J Anim Sci 2011;89:1092–107.
Au J, Choi J, Jones SW, Venkataramanan KP, Antoniewicz MR. Parallel labeling experiments validate clostridium acetobutylicum metabolic network model for 13c metabolic flux analysis. Metab Eng 2014;26:23–33.
Bevans DW, Beauchemin KA, Schwartzkopf-Genswein KS, Mckinnon JJ, Mcallister TA. Effect of rapid or gradual grain adaptation on subacute acidosis and feed intake by feedlot cattle. J Anim Sci 2005;83:1116–32.
Bolger AM, Lohse M, Usadel B. Trimmomatic: a flexible trimmer for illumina sequence data. Bioinformatics 2014;30:2114–20.
Brown MS, Ponce CH, Pulikanti R. Adaptation of beef cattle to high-concentrate diets: performance and ruminal metabolism. J Anim Sci 2006;84(Suppl):E25–33.
Chen L, Shen Y, Wang C, Ding L, Zhao F, Wang M, Fu J, Wang H. Megasphaera elsdenii lactate degradation pattern shifts in rumen acidosis models. Front Microbiol 2019;10:162.
Chen LM, Wang HR. Advances in the metabolism and regulation of lactic acids in the rumen. Pratacult Sci 2016;33:972–80.
Counotte GH, Prins RA, Janssen RH, Debie MJ. Role of megasphaera elsdenii in the fermentation of dl-[2-c]lactate in the rumen of dairy cattle. Appl Environ Microbiol 1981;42:649–55.
Edwards JE, Huws SA, Kim EJ, Lee MR, Kingston-Smith AH, Scollan ND. Advances in microbial ecosystem concepts and their consequences for ruminant agriculture. Animal 2008;2:653–60.
Even S, Lindley ND, Loubiere P, Cocaign-Bousquet M. Dynamic response of catabolic pathways to autoacidification in lactococcus lactis: transcript profiling and stability in relation to metabolic and energetic constraints. Mol Microbiol 2002;45:1143–52.
Fernando SC, Purvis HT, Najar FZ, Sukharnikov LO, Krehbiel CR, Nagaraja TG, Roe BA, Desilva U. Rumen microbial population dynamics during adaptation to a high-grain diet. Appl Environ Microbiol 2010;76:7482–90.
Fu L, Niu B, Zhu Z, Wu S, Li W, Cd-hit. Accelerated for clustering the next-generation sequencing data. Bioinformatics 2012;28:3150–2.
Garvie EI. Bacterial lactate dehydrogenases. Microbiol Rev 1980;44:106–39.
Gilmour M, Mitchell WJ, Flint HJ. Genetic transfer of lactate-utilizing ability in the rumen bacterium selenomonas ruminantium. Lett Appl Microbiol 1996;22:52–6.
Guindon S, Dufayard JF, Lefort V, Anisimova M, Hordijk W, Gascuel O. New algorithms and methods to estimate maximum-likelihood phylogenies: assessing the performance of phyml 3.0. Syst Biol 2010;59:307–21.
Henderson G, Cox F, Ganesh S, Jonker A, Young W, Global Rumen Census C, Janssen PH. Erratum: rumen microbial community composition varies with diet and host, but a core microbiome is found across a wide geographical range. Sci Rep 2016;6:19175.
Hernandez JD, Scott PT, Shephard RW, Al Jassim RA. The characterization of lactic acid producing bacteria from the rumen of dairy cattle grazing on improved pasture supplemented with wheat and barley grain. J Appl Microbiol 2008;104:1754–63.
Hook SE, Steele MA, Northwood KS, Dijkstra J, France J, Wright AD, Mcbride BW. Impact of subacute ruminal acidosis (sara) adaptation and recovery on the density and diversity of bacteria in the rumen of dairy cows. FEMS Microbiol Ecol 2011;78:275–84.
Humer E, Petri RM, Aschenbach JR, Bradford BJ, Penner GB, Tafaj M, Sudekum KH, Zebeli Q. Invited review: practical feeding management recommendations to mitigate the risk of subacute ruminal acidosis in dairy cattle. J Dairy Sci 2018;101:872–88.
Jami E, Mizrahi I. Composition and similarity of bovine rumen microbiota across individual animals. PLoS One 2012;7:e33306.
Kang DD, Li F, Kirton E, Thomas A, Egan R, An H, Wang Z. Metabat 2: an adaptive binning algorithm for robust and efficient genome reconstruction from metagenome assemblies. PeerJ 2019;7:e7359.
Kato O, Youn JW, Stansen KC, Matsui D, Oikawa T, Wendisch VF. Quinone-dependent d-lactate dehydrogenase dld (cg1027) is essential for growth of corynebacterium glutamicum on d-lactate. BMC Microbiol 2010;10:321.
Katoh K, Standley DM. Mafft multiple sequence alignment software version 7: improvements in performance and usability. Mol Biol Evol 2013;30:772–80.
Konings WN, Lolkema JS, Bolhuis H, Van Veen HW, Poolman B, Driessen AJ. The role of transport processes in survival of lactic acid bacteria. Energy transduction and multidrug resistance. Antonie Leeuwenhoek 1997;71:117–28.
Kopylova E, Noe L, Touzet H. Sortmerna: fast and accurate filtering of ribosomal rnas in metatranscriptomic data. Bioinformatics 2012;28:3211–7.
Langmead B, Salzberg SL. Fast gapped-read alignment with bowtie 2. Nat Methods 2012;9:357–9.
Li D, Liu CM, Luo R, Sadakane K, Lam TW. Megahit: an ultra-fast single-node solution for large and complex metagenomics assembly via succinct de bruijn graph. Bioinformatics 2015;31:1674–6.
Li F, Guan Le L, Mcbain Andrew J. Metatranscriptomic profiling reveals linkages between the active rumen microbiome and feed efficiency in beef cattle. Appl Environ Microbiol 2017;83. e00061-17.
Long M, Pang XY, Zhu LQ, Xing X, Liu GW, Wang Z. Isolation and identification of the acid-tolerant lactobacilli from the rumen of a yong cattle. Chin J Vet Sci 2009:288–91.
Macy JM, Ljungdahl LG, Gottschalk G. Pathway of succinate and propionate formation in bacteroides fragilis. J Bacteriol 1978;134:84–91.
Menzel P, Ng KL, Krogh A. Fast and sensitive taxonomic classification for metagenomics with kaiju. Nat Commun 2016;7:11257.
Moriya Y, Itoh M, Okuda S, Yoshizawa AC, Kanehisa M. Kaas: an automatic genome annotation and pathway reconstruction server. Nucleic Acids Res 2007;35:182–5.
Mullins EA, Francois JA, Kappock TJ. A specialized citric acid cycle requiring succinyl-coenzyme a (coa):Acetate coa-transferase (aarc) confers acetic acid resistance on the acidophile acetobacter aceti. J Bacteriol 2008;190:4933–40.
Mullins EA, Kappock TJ. Crystal structures of acetobacter aceti succinyl-coenzyme a (coa):Acetate coa-transferase reveal specificity determinants and illustrate the mechanism used by class i coa-transferases. Biochemistry 2012;51:8422–34.
Nagaraja TG, Titgemeyer EC. Ruminal acidosis in beef cattle: the current microbiological and nutritional outlook. J Dairy Sci 2007;90(Suppl 1):E17–38.
Nocek JE. Bovine acidosis: implications on laminitis. J Dairy Sci 1997;80:1005–28.
Ogunade I, Pech-Cervantes A, Schweickart H. Metatranscriptomic analysis of subacute ruminal acidosis in beef cattle. Animals (Basel) 2019;9:1–12.
Olm MR, Brown CT, Brooks B, Banfield JF. Drep: a tool for fast and accurate genomic comparisons that enables improved genome recovery from metagenomes through de-replication. ISME J 2017;11:2864–8.
Papadimitriou K, Alegria A, Bron PA, De Angelis M, Gobbetti M, Kleerebezem M, Lemos JA, Linares DM, Ross P, Stanton C, Turroni F, Van Sinderen D, Varmanen P, Ventura M, Zuniga M, Tsakalidou E, Kok J. Stress physiology of lactic acid bacteria. Microbiol Mol Biol Rev 2016;80:837–90.
Parks DH, Imelfort M, Skennerton CT, Hugenholtz P, Tyson GW. Checkm: assessing the quality of microbial genomes recovered from isolates, single cells, and metagenomes. Genome Res 2015;25:1043–55.
Pinchuk GE, Rodionov DA, Yang C, Li X, Osterman AL, Dervyn E, Geydebrekht OV, Reed SB, Romine MF, Collart FR, Scott JH, Fredrickson JK, Beliaev AS. Genomic reconstruction of shewanella oneidensis mr-1 metabolism reveals a previously uncharacterized machinery for lactate utilization. Proc Natl Acad Sci U S A 2009;106:2874–9.
Plaizier JC, Danesh Mesgaran M, Derakhshani H, Golder H, Khafipour E, Kleen JL, Lean I, Loor J, Penner G, Zebeli Q. Review: enhancing gastrointestinal health in dairy cows. Animal 2018;12:s399–418.
Plaizier JC, Krause DO, Gozho GN, Mcbride BW. Subacute ruminal acidosis in dairy cows: the physiological causes, incidence and consequences. Vet J 2008;176:21–31.
Rho M, Tang H, Ye Y. Fraggenescan: predicting genes in short and error-prone reads. Nucleic Acids Res 2010;38:e191.
Russell JB, Dombrowski DB. Effect of ph on the efficiency of growth by pure cultures of rumen bacteria in continuous culture. Appl Environ Microbiol 1980;39:604–10.
Tan KH, Seers CA, Dashper SG, Mitchell HL, Pyke JS, Meuric V, Slakeski N, Cleal SM, Chambers JL, Mcconville MJ, Reynolds EC. Porphyromonas gingivalis and treponema denticola exhibit metabolic symbioses. PLoS Pathog 2014;10:e1003955.
Van Soest PJ, Robertson JB, Lewis BA. Methods for dietary fiber, neutral detergent fiber, and nonstarch polysaccharides in relation to animal nutrition. J Dairy Sci 1991;74:3583–97.
Xue M, Sun H, Wu X, Guan LL, Liu J. Assessment of rumen microbiota from a large dairy cattle cohort reveals the pan and core bacteriomes contributing to varied phenotypes. Appl Environ Microbiol 2018;84:1–13.

Yang W, Shen Z, Martens H. An energy-rich diet enhances expression of na(+)/h(+) exchanger isoform 1 and 3 messenger rna in rumen epithelium of goat. J Anim Sci 2012;90:307–17.
Zhao R, Zheng S, Duan C, Liu F, Yang L, Huo G. Nad-dependent lactate dehydrogenase catalyses the first step in respiratory utilization of lactate by lactococcus lactis. FEBS Open Bio 2013;3:379–86.
Zhou XQ, Zhang YD, Zhao M, Zhang T, Zhu D, Bu DP, Wang JQ. Effect of dietary energy source and level on nutrient digestibility, rumen microbial protein synthesis, and milk performance in lactating dairy cows. J Dairy Sci 2015;98:7209–17.